

Landslides (2022) 19:2021–2032  
 DOI 10.1007/s10346-022-01849-z  
 Received: 22 September 2021  
 Accepted: 24 January 2022  
 Published online: 1 April 2022  
 © Springer-Verlag GmbH Germany,  
 part of Springer Nature 2022

Yulong Zhu · Tatsuya Ishikawa · Yafen Zhang · Binh T. Nguyen ·  
 Srikrishnan Siva Subramanian



## A FEM-MPM hybrid coupled framework based on local shear strength method for simulating rainfall/runoff-induced landslide runout

**Abstract** Limited by the independence and its defects of each general software package, simultaneous analysis of runoff, seepage, and large-deformation analysis is still an inevitable challenge. Generally, one of seepage, landslide-related large-deformation, and runoff is ignored or indirectly assessed during unsaturated soil landslide runout simulation. To provide a brand new solution, this paper declares a local shear strength (LSS) method to evaluate rainfall/runoff-induced reduction of the unsaturated soil shear strength. After that, a hybrid coupled hydro-mechanical framework is proposed to simulate rainfall/runoff-induced landslide runout within an unsaturated soil slope. The decrease in local shear strength corresponding to the decrease in matric suction is defined by shifting the Mohr–Coulomb (M-C) failure envelope towards compressive stress space during rainfall/runoff infiltration. Based on the proposed local shear strength method, the variable matric suction obtained from the bidirectionally coupled runoff and seepage analysis in FEM is unidirectionally transferred to the variable local shear strength for each soil material point in MPM (i.e., this is a FEM-MPM hybrid coupled model). Then, the correctness of the proposed hybrid coupled hydro-mechanical framework is effectively verified by a hypothetical homogeneous slope model. The results show that the slope stable/unstable state simulated by the proposed hybrid coupled hydro-mechanical framework has a good consistency with that simulated by the shear strength reduction technique (SSRT) and limit-equilibrium method (LEM). Afterward, combined with a case study of a natural landslide in Hokkaido, Japan, it is proved to be effective for simulating landslide runout subjected to rainfall/runoff infiltration by using the proposed hybrid coupled hydro-mechanical framework in an unsaturated soil slope.

**Keywords** Local shear strength method · Material point method · Rainfall/runoff-induced landslide runout · Finite element method · Unsaturated soil slope

### Introduction

In many mountainous regions, rainfall/runoff is considered to be the main cause triggering landslides/slope failures. With the intensification of global and regional climate change, extreme rainfall events and huge flooding have occurred frequently in recent years (Paerl et al. 2020; Wei et al. 2020). The decrease in matric suction in the unsaturated zone caused by rainwater infiltration under torrential rain is considered the main cause of the landslide/slope failure initiation (Zhu et al. 2020). After the landslide/slope failure occurs, the

collapsed soil moves downward, namely, landslide runout, threatening the lives and properties of residents living downslope, especially those living near the foothills. Therefore, it is of great social and economic value to study the landslide runout distance, reasonably install the disaster prevention measures and set the evacuation area. Many scholars have made great efforts to develop numerical methods for simulating landslide runout, e.g., discrete element method (DEM) (An et al. 2021), discontinuous deformation analysis (DDA) (Shi 1989; Peng et al. 2020), and material point method (MPM) concurrently researched and operated by several groups (Müller and Vargas 2019; Acosta et al. 2021; Sun et al. 2021; Ying et al. 2021). Among them, DEM and DDA consider the geo-material as discrete blocks connected by spring units. Though DEM and DDA are recognized as having the advantages to simulate the cracking behaviors of continuous media or model the contact, collision, slipping, and movement of discretely stacked materials, these two methods also suffer from low convergence, low accuracy, high calibration requirements, and high computational costs. Besides, runoff and seepage analysis are still considered the main limitations of them. Furthermore, a depth-integrated continuum method that uses continuum to model landslide mobility is recently developed by Iverson et al. (2015), Ouyang et al. (2017), and Ouyang et al. (2019). In this method, integrated by the Navier–Stokes equations and flow depth, the mass and momentum equations are solved by using the finite difference method. Apart from these, another method, MPM, is also getting continued attention since it was first formulated by Sulsky et al. (1994), as it avoids the problem of mesh distortion problems in the FEM and shows higher computing efficiency compared with DEM and DDA. In MPM, the material bodies are represented by a large number of material points. The physical information (velocity, acceleration, mass, etc.) is stored in those material points. During the computational process of MPM, the physical information will be repeatedly converted between the background grid and the material points to form a link between the physical information and the spatial position.

The single-phase (solid phase) MPM has been maturely adapted to simulate landslides without considering hydrology. For example, Sun et al. (2015) validated the applicability of the MPM in simulating runout according to the comparative results of experiments and simulations of a simple landslide example. Woo and Rodrigo (2018) presented a generalized interpolation MPM to get higher computational accuracy and efficiency of MPM. Li et al. (2020) simulated the landslide debris movement, and the interaction between landslide debris and baffle structures using 3D MPM model. Recently, MPM has also been developed to capture the rapid landslide behavior in the form of

a soil–water mixture. The porous solid phase, pore water phase, and/or pore air phase are characterized by using two or more Lagrangian layers, i.e., two-phase MPM or multi-phase MPM (e.g., Soga et al. 2016; Liang et al. 2020; Lei et al. 2021). However, it is worth noting that the objects of the above research are mainly rainfall-induced landslides/slope failures in saturated soil or unsaturated soil. The runoff analysis with changes in water depth is neglected since it is considered as one of the fundamental challenges when using either single-phase and two-phase MPM or multi-phase MPM. From the view of the coupling process of runoff and seepage and the variation of matric suction in unsaturated soil, the traditional numerical method, FEM, has more advantages than other methods. Furthermore, it has been widely used in general commercial software packages, which are designed to analyze runoff and/or seepage. For example, COMSOL Multiphysics (COMSOL Multiphysics 2018) and GEO-SEEP/W (GeoStudio International 2007). Therefore, proposing a FEM-MPM coupled computational framework will give full play to their respective advantages in the coupled simulation of runoff, seepage, and landslide runout.

Consequently, the objective of this study was to establish a coupled hydro-mechanical framework to simulate landslide runout triggered by rainfall/runoff infiltration within an unsaturated slope. To achieve this goal, this study firstly proposes a local shear strength method for defining the variation of the local shear strength induced by the rainfall/runoff infiltration for each soil material point. Then, based on the proposed local shear strength method, a hybrid coupled hydro-mechanical framework is developed. In the hybrid coupled hydro-mechanical framework, the seepage behavior is captured by bidirectionally coupled runoff and seepage analysis with the FEM. Then, the variable matric suction obtained from FEM is unidirectionally transferred to the variable local shear strength of each soil material point in MPM by using the local shear strength method. The resulting slope failure behavior is analyzed by the MPM. Thus, a FEM-MPM hybrid coupled model is established. Finally, through a validation model and a case study of a natural slope, the results proved that the proposed FEM-MPM hybrid coupled model is effective for coupled simulating runoff, seepage, and large-deformation problems, such as rainfall/runoff-induced landslide runout within an unsaturated slope.

### Definition of local shear strength for each unsaturated soil material point

The saturated soil shear strength for each material point is defined by the M-C failure criterion:

$$\tau_f = c' + \sigma' \tan\phi' \tag{1}$$

where  $\tau_f$  is the shear strength (kPa);  $c'$  is the effective cohesion (kPa);  $\phi'$  is the effective internal friction angle ( $^\circ$ );  $\sigma'$  is the effective normal stress on failure plane (kPa).

In reality, the soil above the phreatic surface is in an unsaturated state. In this state, the soil will have higher shear strength than in a saturated state. Currently, the well-known method is to describe the unsaturated soil behavior by using Bishop's effective stress concept (Bishop 1959):

$$\sigma' = (\sigma - u_a)_f + \chi(u_a - u_w)_f, \chi = \frac{S_e - S_r}{1 - S_r} \tag{2}$$

where  $u_a$  is pore air pressure (kPa);  $u_w$  is pore water pressure (kPa);  $\sigma$  is total normal stress (kPa);  $\chi$  is effective stress parameter;  $S_e$  is effective degree of saturation;  $S_r$  is residual degree of saturation.

The unsaturated soil shear strength is also defined by Fredlund et al. (1978):

$$\tau_f = c' + (\sigma - u_a)_f \tan\phi' + (u_a - u_w)_f \tan\phi^b \tag{3}$$

where  $\phi^b$  is the angle indicating the rate of increase in shear strength relative to the matric suction  $(u_a - u_w)_f$ .

Equations (2) and (3) present proper compliance with in-door test results and have been widely used (Vanapalli et al. 1996). Vanapalli et al. (1996) discussed the applicability of the above two shear strength models in geotechnical engineering practice and built the relationship between the two models:

$$\chi = \frac{\tan\phi^b}{\tan\phi'} \tag{4}$$

Therefore, the unified equation form can be written as

$$\tau_f = c' + (\sigma - u_a)_f \tan\phi' + (u_a - u_w)_f \chi \tan\phi' \tag{5}$$

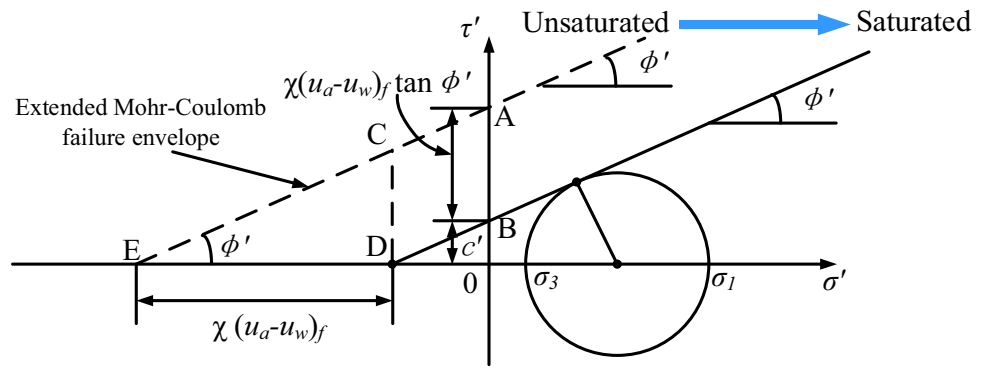
which also can be written as

$$\tau_f = \underbrace{[c' + (u_a - u_w)_f \chi \tan\phi']}_{c'_f} + (\sigma - u_a)_f \tan\phi' \tag{6}$$

where  $c'_f$  is the intercept at a specific matric suction,  $(u_a - u_w)_f$  (kPa).

Conventionally, the M-C failure envelope is fixed for the entire slope during rainfall infiltration. Changes in pore water pressure caused by rainfall/runoff infiltration only affect the scaling and translation of the stress circle. Meanwhile, at present, describing the difference in matric suction induced by runoff of various material points is still a potential challenge of the MPM. Therefore, according to Eq. (6), the variation of local shear strength for each material point in MPM can be described by including matric suction in the cohesion intercept. The new cohesion intercept,  $c'_f$ , is called the total cohesion intercept. This provides a feasible way to define the variation of matric suction and local shear strength for each soil material point in the unsaturated region, as cohesion is one of the material properties that must be assigned during the modeling process. Equation (6) suggests that a decrease in local shear strength (the intercept of the M-C failure envelope decrease) corresponding to a decrease in matric suction during rainfall/runoff infiltration is defined by shifting the M-C failure envelope towards compressive stress space as illustrated in Fig. 1. Consequently, the influences of matric suction changes on the variation of the local shear strength of each soil material point in the unsaturated region can be considered by using the proposed local shear strength method, as shown in Fig. 1.

**Fig. 1** Local shear strength (LSS) for each unsaturated material point



### Hybrid coupled hydro-mechanical framework and governing equations

Based on the proposed local shear strength method, this section firstly proposes a hybrid coupled hydro-mechanical framework of FEM and MPM to simulate runoff, seepage, and large deformation of the unsaturated soil slope. Then, the governing equations used in the runoff model, seepage model, and soil mechanics model are presented.

#### Hybrid coupled hydro-mechanical framework

During a rainstorm or torrential rain, the generation of runoff has a significant impact on soil moisture, ground surface erosion, and landslides. Meanwhile, in unsaturated soils, the variation of volumetric water content affects matric suction, which thereby affects local shear strength. It also affects the self-weight and stress distribution. Therefore, the effects of runoff on the soil moisture changes, and the effects of soil moisture changes on local shear strength and self-weight of unsaturated soil, are considered in the coupled hydro-mechanical framework. In the hybrid coupled hydro-mechanical framework, the runoff and seepage are simulated by using the PDE (partial differential equation) module in the FEM software, COMSOL Multiphysics (COMSOL Multiphysics 2018), while the large-deformation of the landslide is

simulated by using MPM3D (an MPM code that was programmed by the group led by Prof. Zhang Xiong at Tsinghua University, <http://comdyn.hy.tsinghua.edu.cn/english/mpm3d>). The coupled hydro-mechanical framework is shown in Fig. 2. The runoff model and seepage model in FEM are bidirectionally coupled through the interaction between surface water and groundwater (infiltration and exfiltration). The water depth calculated from the runoff model is applied to the seepage model as the water head boundary condition. The inflow velocity (infiltration) and outflow velocity (exfiltration) calculated from the seepage model is returned to the runoff model as the source of water. The coupling process is described in detail elsewhere (Zhu et al. 2020). The FEM analysis and MPM analysis are unidirectionally coupled in two means (1) the influence of changes in soil moisture content (FEM output) on self-weight (MPM input) is taken into account in the elastoplastic model, and (2) the influence of matric suction (FEM output) on the local shear strength (MPM input) is considered by using the local shear strength method. It is worth noting that, as shown in Fig. 2, the proposed FEM-MPM coupled model is not a fully coupled model but a hybrid coupled model. Runoff and seepage analysis is bidirectionally coupled through infiltration and exfiltration in the FEM analysis, while the FEM analysis provides inputs to the MPM analysis, meaning that this process is unidirectionally coupled. Furthermore, under the proposed framework, during the long-term coupled runoff and seepage analysis, it is assumed that the deformation of the slope is not considered because the slope remains stable at this time. While during the large-deformation analysis, when the landslide occurs, the change of seepage force, shear strength, and pore water pressure are neglected as slope failure is a quickly triggered and rapidly developing geological hazard. Therefore, these assumptions are the limitations of the proposed coupled hydro-mechanical framework.

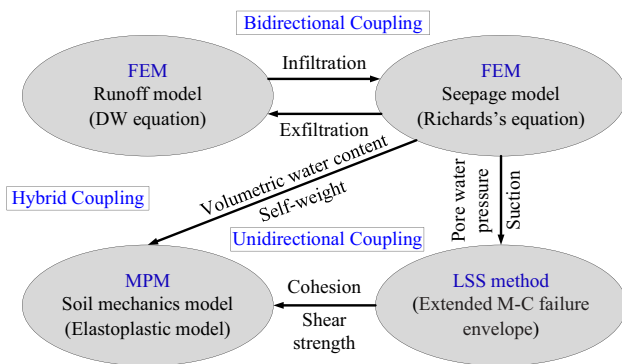


**Fig. 2** Hybrid coupled hydro-mechanical framework of FEM and MPM

#### Governing equation for runoff analysis

Runoff analysis is governed by the diffusion wave (DW) equation as shown in Eq. (7) (Weill et al. 2009; Zhu et al. 2020)

$$\frac{\partial h}{\partial t} - \nabla \left( \frac{h^{5/3}}{n_m \sqrt{|S|}} \nabla(H) \right) = R - I \quad (7)$$

where  $I$  is infiltration/exfiltration rate (m/s);  $t$  is time (s);  $n_m$  is Manning's roughness coefficient ( $s/m^{1/3}$ );  $h$  is runoff depth (m);  $H$  is water surface elevation (m);  $R$  is rainfall intensity (m/s);  $S$  is water surface gradient, which can be replaced by slope gradient due to the small difference between them (Weill et al. 2009).

**Governing equation for seepage analysis**

Seepage analysis is governed by the equation proposed by Richards (1931), which can be expressed as follows:

$$\nabla \cdot [k_s k_r \cdot \nabla (H_p + z)] + Q_w = [C_m + S_e S_c] \frac{\partial H_p}{\partial t} \tag{8}$$

where  $Q_w$  is sink and source of water ( $s^{-1}$ ), which is related to  $I$ ;  $k_s$  is saturated hydraulic conductivity (m/s);  $C_m$  is specific moisture capacity ( $m^{-1}$ );  $k_r$  is relative hydraulic conductivity;  $S_c$  is specific storage coefficient ( $m^{-1}$ );  $H_p$  is pressure head (m);  $S_e$  is the effective degree of saturation;  $z$  is the elevation (m). The relationship in  $C_m$ ,  $S_e$ ,  $k_r$ ,  $\theta$ , and  $H_p$  in unsaturated soil can be calculated by  $\theta_s$ ,  $\theta_r$ , and the vG parameters,  $a$ ,  $n$ ,  $m$ , and  $l$  (van Genuchten 1980).

$$\theta = \theta_r + S_e (\theta_s - \theta_r) \tag{9}$$

$$S_e = \frac{1}{[1 + (aH_p)^n]^m}, m = 1 - \frac{1}{n} \tag{10}$$

$$C_m = \frac{am}{1-m} (\theta_s - \theta_r) S_e^{\frac{1}{m}} (1 - S_e^{\frac{1}{m}})^m \tag{11}$$

$$k_r = S_e^l \left[ 1 - (1 - S_e^{\frac{1}{m}})^m \right]^2 \tag{12}$$

**Governing equations in MPM**

In MPM, each computational step can be divided into three phases: initial phase, Lagrangian phase, and convective phase, as shown in Fig. 3 (Sun et al. 2015). In the initial phase, the physical information stored in material points (e.g., locations, velocities, mass, etc.) is mapped on the Lagrangian background grid to get the initial solution values. In the Lagrangian phase, the material points move

with the Lagrangian background grid, and the global equations are solved within the Lagrangian background grid. After that, the stored physical information is updated. In the convective phase, the Lagrangian background grid is reset, while the stored physical information remains unchanged.

The governing equations of large-deformation analysis in MPM can be expressed as follows (Abe et al. 2013):

$$\frac{d\rho(\theta)}{dt} + \rho(\theta) \nabla \cdot \mathbf{v} = 0 \text{ (conservation of mass)} \tag{13}$$

$$\rho(\theta) \mathbf{a} = \nabla \cdot \boldsymbol{\sigma} + \rho(\theta) \mathbf{b} \text{ (conservation of momentum)} \tag{14}$$

where  $\rho(\theta)$  is soil-water mixture density ( $kg/m^3$ ) as a function of volumetric water content ( $\theta$ );  $\mathbf{a}$  is acceleration vector ( $m/s^2$ );  $\mathbf{v}$  is velocity vector (m/s);  $\mathbf{b}$  is body forces vector ( $m/s^2$ );  $\boldsymbol{\sigma}$  is stress tensor (kPa).

**Validation of the proposed hybrid coupled hydro-mechanical framework**

To check the reliability of the hybrid coupled hydro-mechanical framework proposed in this study for simulating unsaturated soil slope instability, a validation model is simulated by the FEM-MPM hybrid coupled model compared with the other two commonly used methods: limit-equilibrium method and shear strength reduction technique. In the validation model, the water supply (rainfall and runoff) is not considered. The two side walls and bottom are impermeable to water. The groundwater level (GWL) is assumed to be  $-5$  m. Table 1 lists the soil properties used in the validation model. The model size and boundary conditions are displayed in Fig. 4. The simulation results of the shear strength reduction technique are obtained from COMSOL, and the simulation results of the limit-equilibrium method are obtained from another commercial slope-stability software package GEO-SLOPE/W (GeoStudio International 2007).

The comparison of the simulation results calculated by shear strength reduction technique, limit-equilibrium method, and the proposed FEM-MPM hybrid coupled model are shown in Fig. 5. Figure 5a shows the slope in the stable state. Figure 5b shows the slope in the critical state. Figure 5c shows the slope in the failure state. In each sub-figure (Fig. 5a-c), Fig. 5(I) displays

**Fig. 3** Three phases of one computational step of MPM (adapted from Sun et al. (2015))

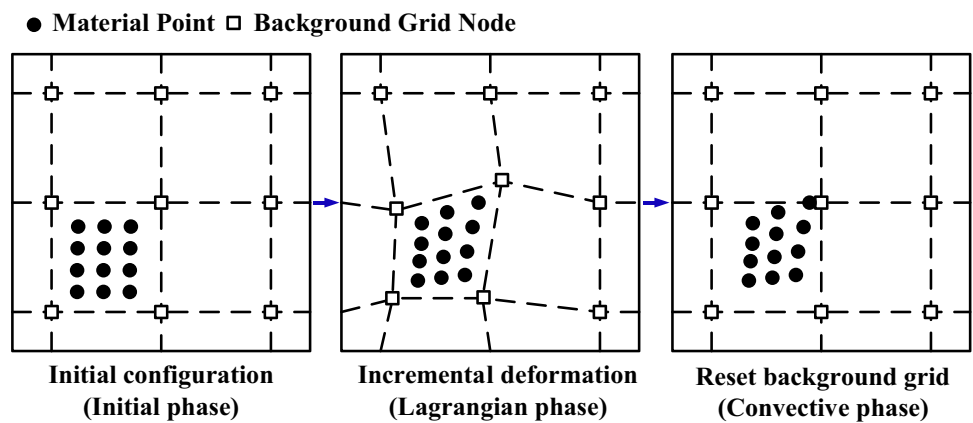


**Table 1** Soil properties used in the validation model

Dry density, $\rho_s$ (kg/m <sup>3</sup> )	Effective cohesion, $c'$ (kPa)	Effective internal friction angle, $\phi'$ (°)	Young's modulus, $E$ (MPa)	Poisson's ratio, $\nu$
1695	0 and 10	20 and 30	50	0.3
Saturated hydraulic conductivity, $k_s$ (m/s)	Saturated vol. water content, $\theta_s$ (m <sup>3</sup> /m <sup>3</sup> )	Residual vol. water content, $\theta_r$ (m <sup>3</sup> /m <sup>3</sup> )	vG parameter, $\alpha$ (1/m)	vG parameter, $m$
$1.12 \times 10^{-5}$	0.36	0.035	0.538	0.468

the pressure head calculated by FEM. Figure 5(II) displays the slip surface simulated by the limit-equilibrium method with the factor of safety (FOS). Figure 5(III) displays the results simulated by the shear strength reduction technique. Figure 5(IV) displays the ultimate slope failure shape simulated by the proposed FEM-MPM hybrid coupled model. From Fig. 5a, it is recognized that the slope simulated by the proposed FEM-MPM hybrid coupled model is stable. The FOS calculated by the limit-equilibrium method (FOS = 1.198) in Fig. 5a(II), and that calculated by the shear strength reduction technique (FOS = 1.190) in Fig. 5a(III) are larger than 1.0. From Fig. 5b, it is recognized that the slope simulated by the proposed FEM-MPM hybrid coupled model is in a critical state. At the same time, the FOS calculated by limit-equilibrium method (FOS = 0.996) in Fig. 5b(II) and that calculated by shear strength reduction technique (FOS = 0.930) in Fig. 5b(III) are slightly less than 1.0, meaning that the slope is unstable under the pore water pressure distribution at this time. From Fig. 5c, it is recognized that the slope simulated by the proposed FEM-MPM hybrid coupled model is failed. The FOS calculated by the limit-equilibrium method (FOS = 0.567) in Fig. 5c(II), and that calculated by the shear strength reduction technique (FOS = 0.590) in Fig. 5c(III) are much less than 1.0. Figure 5a–c indicates that the slope stable/unstable state simulated by the proposed FEM-MPM hybrid coupled model is consistent with that calculated by the limit-equilibrium method and the shear strength reduction technique. The similar slip surface shapes and stable/unstable state calculated by the proposed FEM-MPM hybrid

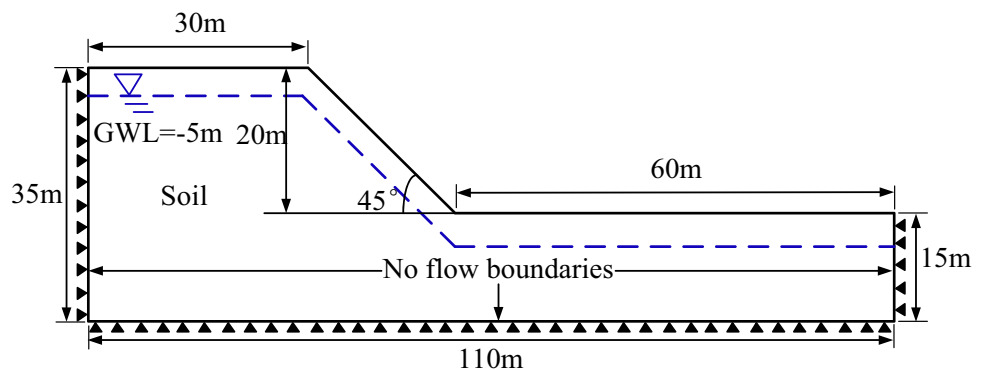
coupled model, limit-equilibrium method, and shear strength reduction technique give a good verification of the proposed FEM-MPM hybrid coupled model on simulating slope instability in unsaturated soil, although the slip surface calculated by shear strength reduction technique is slightly shallower in Fig. 5b, c. The main reason could be that the slip surface calculated by the shear strength reduction technique is the initial slip surface. Due to the calculation of the shear strength reduction technique being terminated due to non-convergence after the shallow layer is damaged, the development process of the slip surface from the initial stage to the ultimate stage is not considered by the shear strength reduction technique.

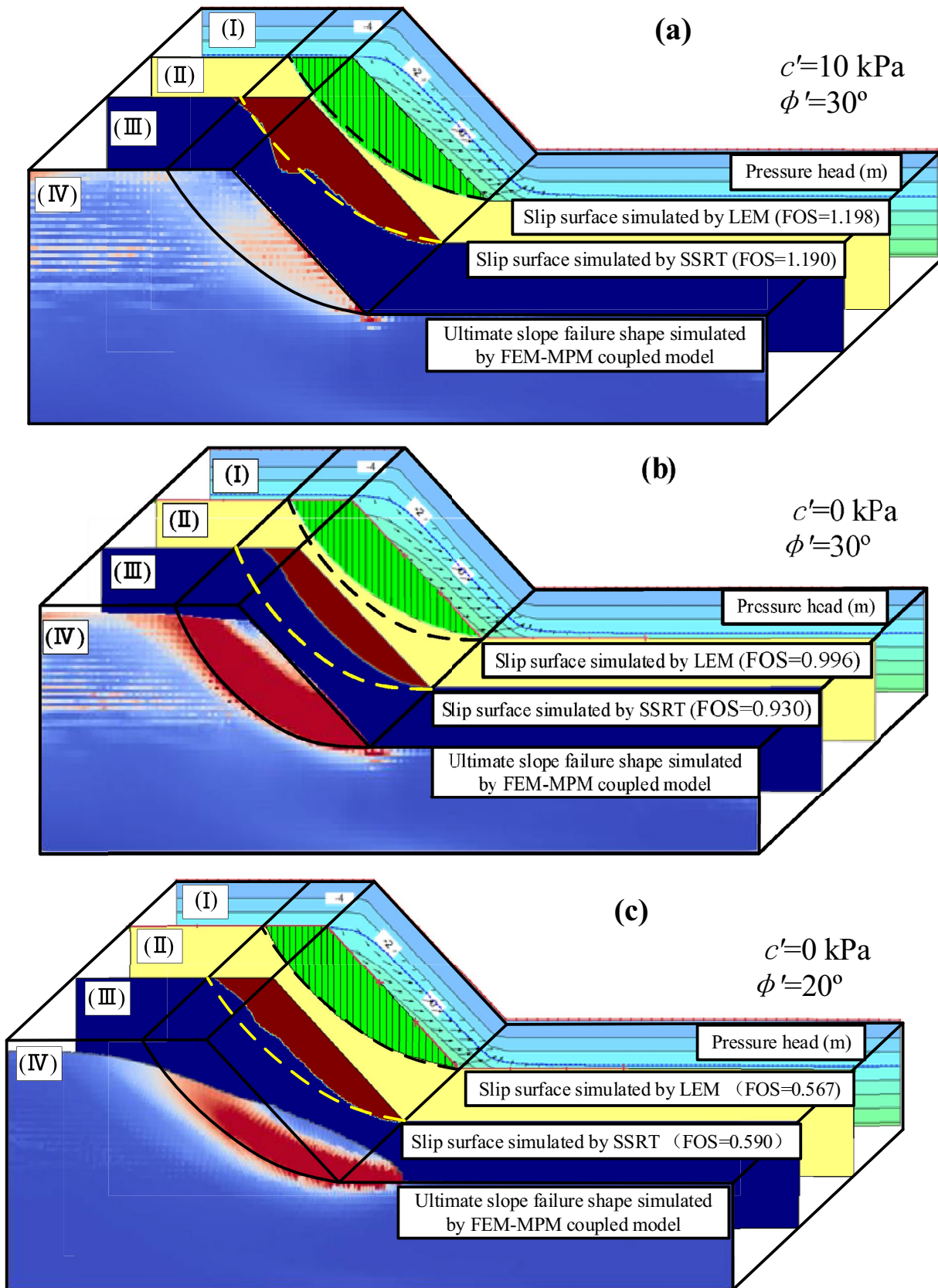
**Natural landslide simulation by the proposed FEM-MPM hybrid coupled model**

**Numerical model and soil properties**

In 2016, typhoon No. 10 hit Northern Japan at the end of August. During this period, several serious landslides occurred, for example, at location 1 in Fig. 6. The landslide is located in the Hidaka mountains in Hokkaido, Japan. The maximum observed cumulative rainfall in 3 days (29<sup>th</sup>–31<sup>st</sup>) reached 488 mm, as plotted in Fig. 7. The geological conditions of this site are dominated by metamorphic rocks and plutonic rocks that belong to the Hidaka metamorphic belt. It is mainly composed of medium-grained and massive granite containing biotite. The shallow part of the granite that penetrates the sedimentary rocks of the Hidaka metamorphic

**Fig. 4** Schematic diagram of the validation model





◀**Fig. 5** Numerical results calculated from limit-equilibrium method, shear strength reduction technique, and FEM-MPM hybrid coupled model. **a** stable state; **b** critical state; **c** failure state. In each sub-figure, (I) pressure head calculated by FEM, (II) slip surface with FOS simulated by limit-equilibrium method, (III) slip surface with FOS simulated by shear strength reduction technique; (IV) ultimate slope failure shape simulated by FEM-MPM hybrid coupled model

belt is being weathered, forming a layer of weathered residual soil about 10 m on the ground surface. Focus on the target area surrounded by the red dashed rectangle in Fig. 6, a three-dimensional (3D) model for runoff and seepage analysis was built as displayed in Fig. 8a. Figure 8b displays the cross-section at location 1. Only one two-dimensional (2D) profile at location 1 was simulated by the MPM model for large-deformation analysis. Figure 8c displays the material points with the number of 10,487 within the 2D profile. More simulations of 2D profiles along the sliding direction are repetitive work, so they are not carried out in this study.

In the 3D model, the geological composition information is shown in Fig. 8a, and it is considered that the embankment exists only at the exit of the valley, and the thickness of the soil is 10 m. Soil properties are listed in Table 2. The parameters i.e., dry density ( $\rho_s$ ), saturated hydraulic conductivity ( $k_s$ ), saturated volumetric water content ( $\theta_s$ ), effective cohesion ( $c'$ ), and effective friction angle ( $\phi'$ ), Young's modulus ( $E$ ), and Poisson's ratio ( $\nu$ ) have been obtained from laboratory element tests (Sato et al. 2017). The parameters for which no results of laboratory tests are available, i.e., residual volumetric water content ( $\theta_r$ ) and van Genuchten parameters ( $\alpha$  and  $m$ ), were estimated based on the grain size curve of soil by using the software, SoilVision (SoilVision 2018). SoilVision is geotechnical database software that contains data on over 6200 soil samples. It can be used to estimate the missing characteristic values of the soil based on the grain size curve of the soil. The initial GWL is set to  $-5.5$  m considering historical measurements. According to the value for mountain grassland recommended by the Japan Institute of Country-ology and Engineering (JICE), Manning's coefficient value is set to  $0.3 \text{ s/m}^{1/3}$ .

**Fig. 6** Locations and performance of slope failure

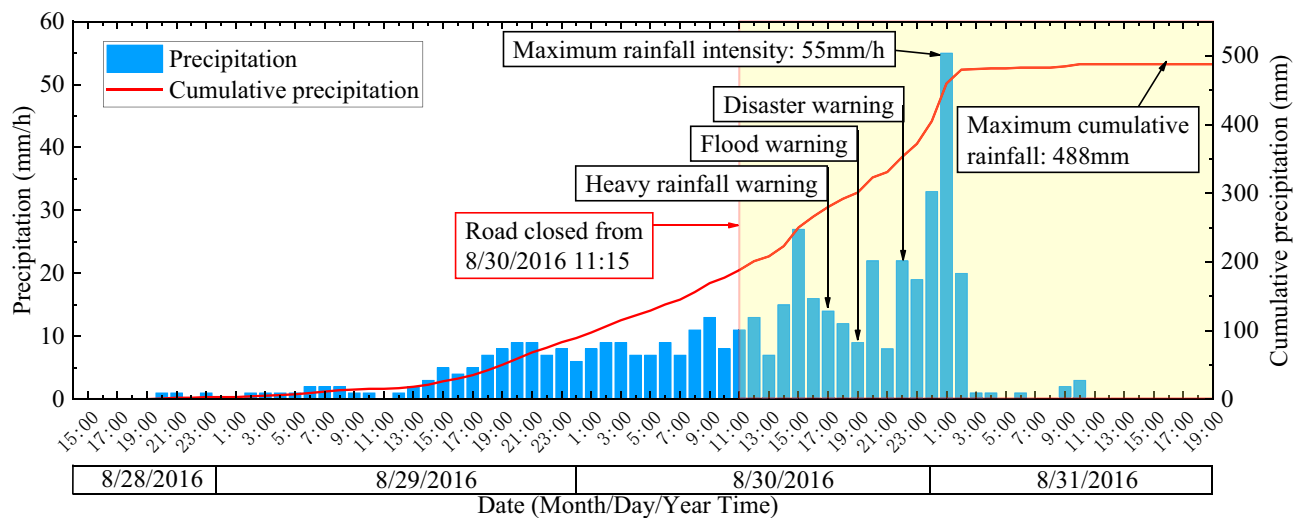
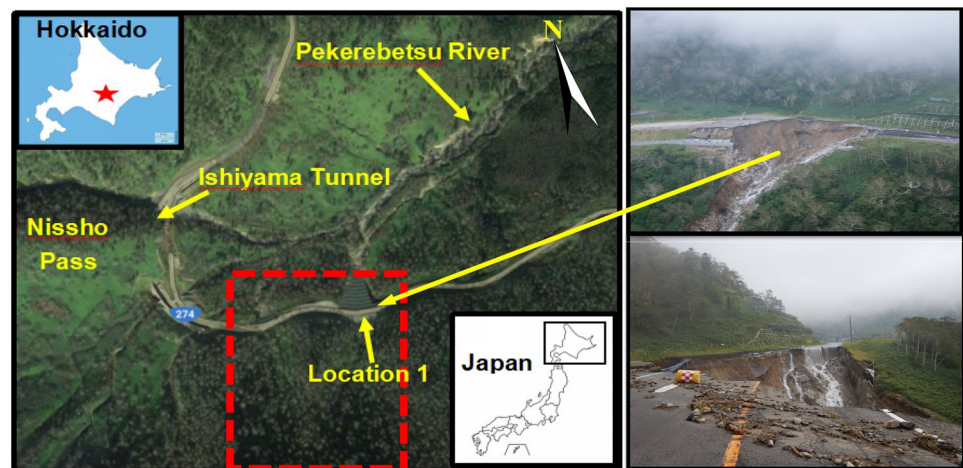


**Fig. 7** Recorded rainfall during typhoon no.10

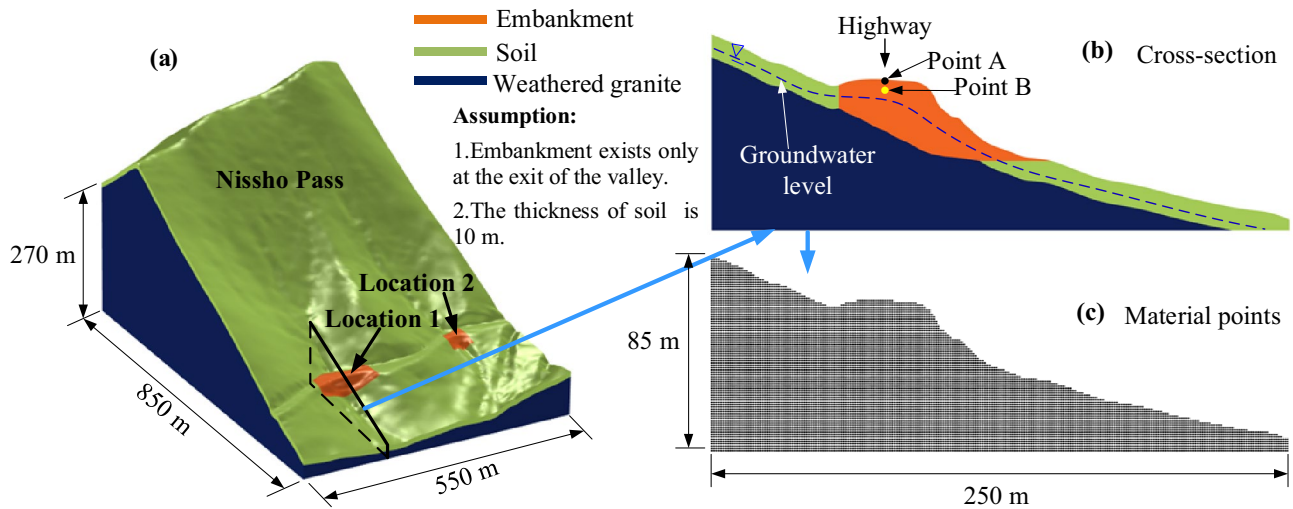


**Fig. 8** a 3D numerical model of the target area; b cross-section at location 1; c material points at location 1

**Table 2** Soil properties used for the FEM-MPM hybrid coupled simulation

Parameters	Dry density, $\rho_s$ (kg/m <sup>3</sup> )	Effective cohesion, $c'$ (kPa)	Effective internal friction angle, $\phi'$ (°)	Young's modulus, $E$ (MPa)	Poisson's ratio, $\nu$
Embankment	1695	0	37	50	0.3
Soil	1020	0	35	50	0.3
Weathered granite	2000	37	21	500	0.3
Parameters	Saturated hydraulic conductivity, $k_s$ (m/s)	Saturated volumetric water content, $\theta_s$ (m <sup>3</sup> /m <sup>3</sup> )	Residual volumetric water content, $\theta_r$ (m <sup>3</sup> /m <sup>3</sup> )	vG parameter, $\alpha$ (1/m)	vG parameter, $m$
Embankment	$1.12 \times 10^{-5}$	0.36	0.035	0.538	0.468
Soil	$1.40 \times 10^{-6}$	0.63	0.190	0.810	0.012
Weathered granite	$3.47 \times 10^{-9}$	0.48	0.008	0.437	0.246

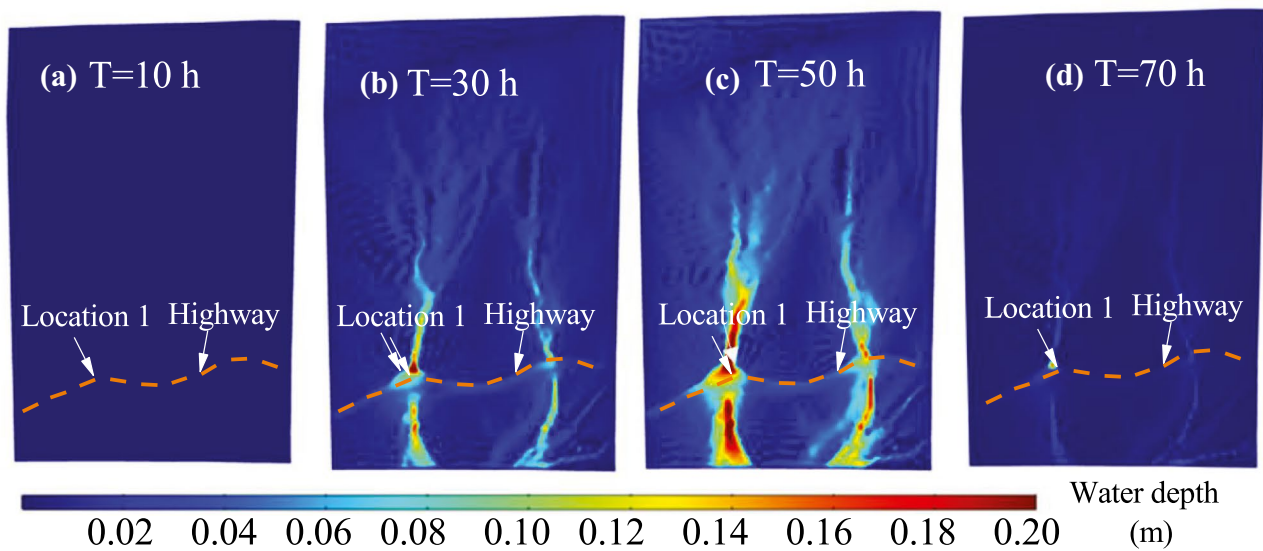


**Fig. 9** Time-dependent water depth distribution at Nissho Pass a at  $T=10$  h; b at  $T=30$  h; c at  $T=50$  h; d at  $T=70$  h



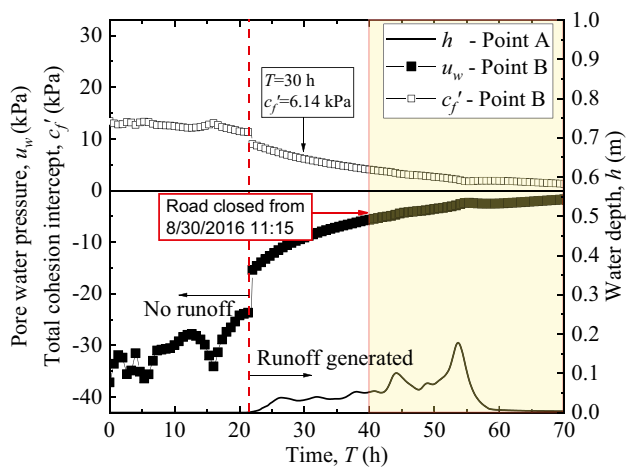


**Fig. 10** Time-dependent water depth ( $h$ ), pore water pressure ( $u_w$ ), and total cohesion intercept ( $c'_f$ )

### Simulation results of the natural landslide induced by runoff

The bidirectionally coupled runoff and seepage analysis are firstly done with FEM. The simulation time (represented by  $T$ ) is a total of 70 h from August 28, 2016 20:00 to August 31, 2016 18:00. The calculation step is set as an adaptive time-stepping scheme that means the COMSOL will automatically adjust the calculation time in each step to meet the desired relative tolerance (0.001 in this

study). The results output time step is 1.0 h. That is after, every hour of the bidirectionally coupled runoff and seepage analysis, the volumetric water content and matric suction obtained from FEM analysis are transferred to the MPM model and used for updating the information of mass self-weight and local shear strength stored in each soil material point. From trial simulations, it is found that from 15 s after the start of the MPM analysis, the slope failure shape does not change significantly even if the calculation time is greatly increased. Therefore, the total time (represented by  $t$ ) for a landslide runout simulation by MPM is set to 15 s, and the calculation step is 0.2 s. Figure 9 shows the distribution of time-dependent water depth in the target area. In Fig. 9, it can be identified that the overland water from the watershed is gathered at location 1 since location 1 is located at the exit of the valley. The water depth exceeds 0.2 m in the upstream area of location 1, which is much larger than other parts of the highway. This was considered the main cause of the landslide that occurred at location 1.

The simulated water depth ( $h$ ) at the road center (Point A in Fig. 8b, located on the road surface), pore water pressure ( $u_w$ ), and total cohesion intercept ( $c'_f$ ) at an exploratory point (point B in Fig. 8b, located at 1.0 m deep below the road surface) are plotted in Fig. 10. From Figs. 9 and 10, it is identified that the generation of runoff is at 22 h after the bidirectionally coupled runoff and seepage analysis starts. After runoff is generated, there is a dramatic increase in  $u_w$  and a sudden drop of  $c'_f$ , meaning that the generation of runoff has a remarkable influence on the matric suction and local shear strength of the embankment. Afterward, the matric suction gradually decreases to close to zero, i.e., the pore water

**Fig. 11** Distribution of time-dependent effective degree of saturation at Nissho Pass **a** at  $T=0$  h; **b** at  $T=30$  h; **c** at  $T=50$  h; **d** at  $T=70$  h

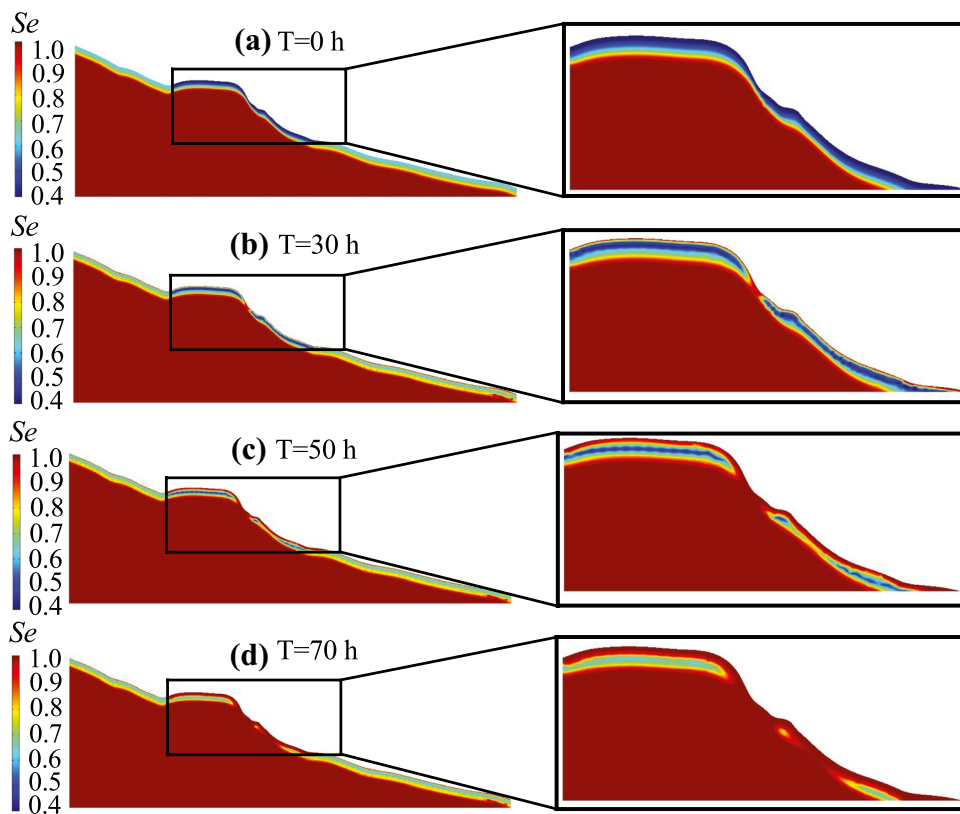
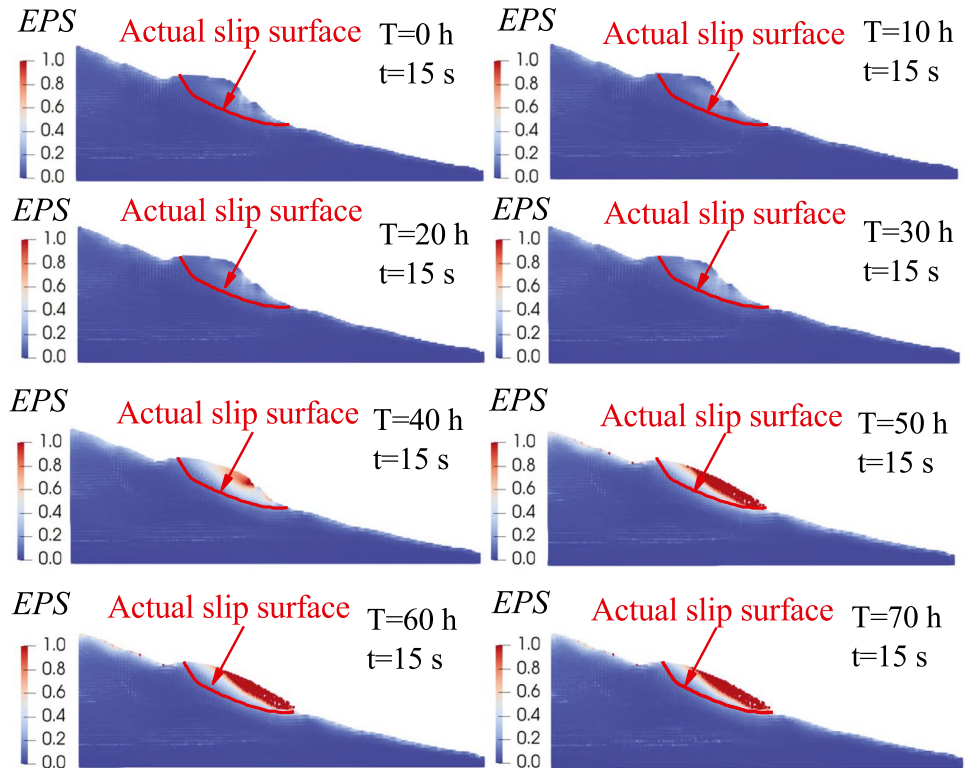


**Fig. 12** Distribution of effective plastic strain and slope failure shape with large deformations at Nissho Pass



pressure ( $u_w$ ) gradually increases to close to zero (soil is nearly saturated), causing a continuous decrease in total cohesion intercept ( $c_f'$ ) of the embankment. The decrease in the total cohesion intercept ( $c_f'$ ) leads to the decrease in the local shear strength, which causes the occurrence of the landslide. Figure 11 shows the effective degree of saturation ( $S_e$ ) at different times. It is recognized that the unsaturated soil lies above the saturated zone. The infiltration of rainwater gradually saturates the soil on the surface layer, thus resulting in the size of the unsaturated zone becoming smaller. It is also identified that after runoff is generated at  $T = 22$  h, the soil on the surface layer becomes saturated at  $T = 30$  h in Fig. 11, and the saturated area gradually increases with time after  $T = 30$  h.

Figure 12 shows the distribution of effective plastic strain (EPS) and slope failure shape with large deformation at 15 s in the landslide simulation. A new MPM analysis has been run for each time with different matric suction and local shear strength outputted from FEM analysis. During the MPM analysis, it is assumed that the matric suction and local shear strength for each point keep constant. The above assumption can be considered reasonable since the calculation of MPM is completed in only 15 s, which is a very short time, so the change of matric suction and local shear strength is neglectable. From Fig. 12, it is recognized that the slope is stable before  $T = 40$  h due to a large size unsaturated zone lies above the saturated zone (see Fig. 11). Though high matric suction causes a high local shear strength of the embankment soil, with the infiltration of rainwater, the matric suction gradually decreases, causing a continuous decrease in local shear strength of the embankment (see Fig. 10). Finally, the slope failure occurred at approximately 40 h (the highway was closed at the same time as shown in Fig. 10) and reached its ultimate shape between 40 and 50 h (slope failure was complete). Therefore, this simulation has also shown the effectiveness of the

proposed hybrid coupled hydro-mechanical framework (FEM-MPM hybrid coupled model) to reproduce and/or predict the rainfall/runoff induced slope failure in unsaturated soil, although the simulated slip surface is shallower compared with the actual one as shown in Fig. 12. The main reason could be that after the occurrence of the landslide, the development of the slip surface caused by the erosion of the newly exposed ground surface by the surface water has not been considered. This needs to be further investigated by considering the continuous erosion of runoff in the proposed FEM-MPM hybrid coupled model, which is one of the limitations of this study currently.

### Discussions and conclusions

This paper proposes a local shear strength method for determining the variable local shear strength corresponding to the variable matric suction for each soil material point within a small catchment-scale unsaturated slope. The local shear strength method built a relationship between the variable local shear strength and the variable matric suction of each soil material point during rainfall/runoff infiltration by shifting the M-C failure envelope.

A hybrid coupled hydro-mechanical framework is proposed based on the local shear strength method to solve rainfall/runoff induced landslide runoff in unsaturated slopes. Based on the hybrid coupled hydro-mechanical framework, a FEM-MPM hybrid coupled model is established. The landslide analysis results suggest that the slope stable/unstable state simulated by the FEM-MPM hybrid coupled model has a good consistency with the slip surface simulated by the limit-equilibrium method and shear strength reduction technique. It is proved to be also reliable to simulate the actual slope failure process to determine the occurrence time and location. Therefore, the proposed FEM-MPM hybrid coupled model

is proved to be applicable for simulating rainfall/runoff-induced unsaturated soil landslide runout and has the potential to understand the location of landslide initiation and the morphological evolution.

These findings indicate that the local shear strength method and hybrid coupled hydro-mechanical framework proposed in this study provide a feasible way to simulate rainfall/runoff-induced landslide runout in unsaturated soil slopes. It is of great significance to evaluate the landslides movement distance and reasonably recommend the installation of barrier structures to protect the lives and properties of residents living downslope. However, the internal moisture changes and the dynamic support provided by the runoff during the movement of the landslide are not considered in this study. These should be considered in the future assignments of this study.

### Acknowledgements

The authors give sincere thanks to Prof. Zhang Xiong at Tsinghua University for the open source MPM3D code. Since the main works of this study were finished at Hokkaido University, the authors gratefully acknowledge the support of Hokkaido University and the Hokkaido Government.

### Funding

This research was supported in part by Grants-in-Aid for Scientific Research (A) (16H02360) from the Japan Society for the Promotion of Science (JSPS) KAKENHI. This research is also supported by the Fundamental Research Funds for the Central Universities (2021MS043).

### Data availability

Weather station data used in this research can be downloaded from Japan Meteorological Agency (<http://www.data.jma.go.jp/gmd/risk/obsdl/index.php>), and terrain information can be got from Geospatial Information Authority of Japan (<https://www.gsi.go.jp/top.html>).

### Declarations

**Competing interests** The authors declare no competing interests.

### References

Abe K, Soga K, Bandara S (2013) Material point Method for coupled hydromechanical problems. *J Geotech Geoenviron Eng* 140(3):04013033

Acosta JLG, Vardon PJ, Hicks MA (2021) Study of landslides and soil-structure interaction problems using the implicit material point method. *Eng Geol* 285:106043

An H, Ouyang C, Zhou S (2021) Dynamic process analysis of the Baige landslide by the combination of DEM and long-period seismic waves. *Landslides* 18(5):1625–1639

Bishop AW (1959) The principle of effective stress. *Teknisk Ukeblad, Norwegian Geotechnical Institute* 106(39):859–863

COMSOL Multiphysics (2018) version 5.4, COMSOL Inc., Sweden

Fredlund DG, Morgenstern NR, Widger RA (1978) The shear strength of unsaturated soils. *Can Geotech J* 15:313–321

GeoStudio International (2007) GEOSLOPE, Calgary, Alberta, Canada

Iverson RM, George DL, Allstadt K et al (2015) Landslide mobility and hazards: implications of the 2014 Oso disaster. *Earth Planet Sci Lett* 412:197–208

Lei X, He S, Abed A, Chen X, Yang Z, Wu Y (2021) A generalized interpolation material point method for modelling coupled thermo-hydro-mechanical problems. *Comput Methods Appl Mech Eng* 386:114080

Li X, Yan Q, Zhao S, Luo Y, Wu Y, Wang D (2020) Investigation of influence of baffles on landslide debris mobility by 3D material point method. *Landslides* 17:1129–1143

Liang D, Zhao X, Soga K (2020) Simulation of overtopping and seepage induced dike failure using two-point MPM. *Soils Found* 60(4):978–988

Müller A, Vargas EA (2019) Correction to: stability analysis of a slope under impact of a rock block using the generalized interpolation material point method (GIMP). *Landslides* 16:1063

Ouyang C, Zhou K, Xu Q et al (2017) Dynamic analysis and numerical modeling of the 2015 catastrophic landslide of the construction waste landfill at Guangming, Shenzhen. *China Landslides* 14(2):705–718

Ouyang C, An H, Zhou S et al (2019) Insights from the failure and dynamic characteristics of two sequential landslides at Baige village along the Jinsha River. *China Landslides* 16(7):1397–1414

Paerl HW, Hall NS, Hounshell AG et al (2020) Recent increases of rainfall and flooding from tropical cyclones (TCs) in North Carolina (USA): implications for organic matter and nutrient cycling in coastal watersheds. *Biogeochemistry* 150(2):197–216

Peng X, Yu P, Chen G, Xia M, Zhang Y (2020) Development of a coupled DDA-SPH method and its application to dynamic simulation of landslides involving solid-fluid interaction. *Rock Mech Rock Eng* 53(1):113–131

Richards LA (1931) Capillary conduction of liquids through porous mediums. *Physics* 1(5):318–333

Sato A, Hayashi T, Hayashi H, Yamaki M (2017) On the geotechnical properties of decomposed granite soil in Hokkaido. 57th Technical Report of Hokkaido Branch of Japanese Geotechnical Society. 145–148. (in Japanese)

Shi GH (1989) Discontinuous deformation analysis a new numerical model for the static and dynamics of block systems. Ph.D. Dissertation, Dept. of Civil Engineering.

Soga K, Alonso E, Yerro A, Kumar K, Bandara S (2016) Trends in large-deformation analysis of landslide mass movements with particular emphasis on the material point method. *Géotechnique* 66(3):248–273

SoilVision (2018) version, 4.23. SoilVision Systems Ltd. Saskatoon, Saskatchewan, Canada

Sulsky D, Chen Z, Schreyer HL (1994) A particle method for history-dependent materials. *Comput Methods Appl Mech Eng* 118(1–2):179–196

Sun F, Wang G, Zhang L, Wang R, Cao T, Ouyang X (2021) Material point method for the propagation of multiple branched cracks based on classical fracture mechanics. *Comput Methods Appl Mech Eng* 386:114116

Sun Y, Yang J, Song E (2015) Runout analysis of landslides using material point method. *Iop Conference Series: Earth and Environmental Science*. IOP Publishing 26(1):012014

van Genuchten MTh (1980) A closed-form equation for predicting the hydraulic conductivity of unsaturated soils. *Soil Sci Soc Am J* 44(5):892–898

Vanapalli SK, Fredlund DG, Pufahl DE, Clifton AW (1996) Model for the prediction of shear strength with respect to soil suction. *Can Geotech J* 33(3):379–392

Wei K, Ouyang C, Duan H, Li Y, Chen M, Ma J, An H, Zhou S (2020) Reflections on the catastrophic 2020 Yangtze River Basin flooding in Southern China. *The Innovation* 1(2):100038

Weill S, Mouche E, Patin J (2009) A generalized Richards equation for surface/subsurface flow modelling. *J Hydrol* 366(1–4):9–20

Woo SI, Rodrigo S (2018) Simulation of penetration of a foundation element in Tresca soil using the generalized interpolation material point method (GIMP). *Comput Geotech* 94:106–117

Ying C, Zhang K, Wang ZN, Siddiqua S, Makeen GMH, Wang L (2021) Analysis of the run-out processes of the Xinlu Village landslide using the generalized interpolation material point method. *Landslides* 18:1519–1529

Zhu Y, Ishikawa T, Subramanian SS, Luo B (2020) Simultaneous analysis of slope instabilities on a small catchment-scale using coupled surface and subsurface flows. Eng Geol 275:105750

---

### Yulong Zhu

School of Water Resources and Hydropower Engineering, North China Electric Power University, Changping Beinong 2#, Beijing, China

### Tatsuya Ishikawa (✉)

Laboratory of Analytical Geomechanics, Faculty of Engineering, Hokkaido University, Kita 13, Nishi 8, Kita-ku, Sapporo, Hokkaido 060-8628, Japan  
Email: t-ishika@eng.hokudai.ac.jp

### Yafen Zhang

School of Engineering, The Open University of China, Haidian Wukesong, Beijing, China

### Binh T. Nguyen

Research and Development Center, Nippon Koei Co., Ltd, 2304 Inarihara, Tsukuba, Ibaraki, Japan

### Srikrishnan Siva Subramanian

Centre of Excellence in Disaster Mitigation and Management, Indian Institute of Technology Roorkee, Roorkee, Uttarakhand 247667, India  
Email: srikrishnan@dm.iitr.ac.in